The Journal of Chemical Physics

A Bayesian approach for identification of ice Ih, ice Ic, high density, and low density liquid water with a torsional order parameter

Cite as: J. Chem. Phys. **150**, 214504 (2019); https://doi.org/10.1063/1.5096556
Submitted: 18 March 2019 . Accepted: 13 May 2019 . Published Online: 05 June 2019

Masakazu Matsumoto, Takuma Yagasaki, and Hideki Tanaka

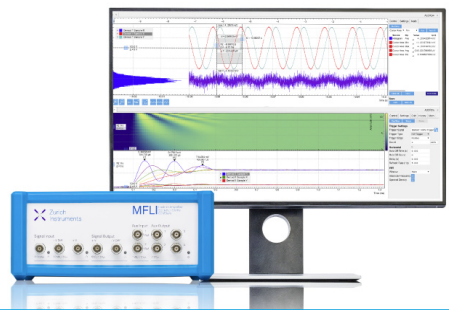

AIP Publishing

The Journal of Chemical Physics ARTICLE scitation.org/journal/jcp

A Bayesian approach for identification of ice Ih, ice Ic, high density, and low density liquid water with a torsional order parameter

Cite as: J. Chem. Phys. 150, 214504 (2019); doi: 10.1063/1.5096556
Submitted: 18 March 2019 • Accepted: 13 May 2019 •
Published Online: 5 June 2019

Masakazu Matsumoto,[a] Takuma Yagasaki,[b] and Hideki Tanaka

AFFILIATIONS

Research Institute for Interdisciplinary Science, Okayama University, Okayama 700-8530, Japan

Note: This paper is part of a JCP Special Topic on Chemical Physics of Supercooled Water.
[a]**Electronic mail:** vitroid@gmail.com
[b]**Electronic mail:** t.yagasaki@gmail.com

ABSTRACT

An order parameter is proposed to classify the local structures of liquid and solid water. The order parameter, which is calculated from the O–O–O–O dihedral angles, can distinguish ice Ih, ice Ic, high density, and low density liquid water. Three coloring schemes are proposed to visualize each of the coexisting phases in a system using the order parameter on the basis of Bayesian decision theory. The schemes are applied to a molecular dynamics trajectory in which ice nucleation occurs following spontaneous liquid-liquid separation in the deeply supercooled region as a demonstration.

INTRODUCTION

Properties of water have been investigated both experimentally and theoretically.[1] Molecular dynamic (MD) simulations of water, which were founded by Rahman and Stillinger, brought us vast knowledge on microscopic characters of water as well as simulation and analysis methods that are applicable to other molecules.[2] Modern sophisticated interaction models of water can reproduce the complicated phase diagram in wide ranges of temperature and pressure and even enable us to predict new phases prior to experiments.[3–10]

It has been anticipated that water exhibits polyamorphism, i.e., existence of multiple noncrystalline condensed phases.[11–14] While it is very difficult to observe spontaneous liquid-liquid separation in bulk water by experiments, molecular dynamics (MD) simulations have succeeded in doing so.[15,16] Although the polyamorphic transition occurs between the metastable liquid phases under deeply supercooled conditions, the critical fluctuations associated with it are considered to affect properties of stable phases of water under ambient conditions. Water is known to have a lot of anomalous properties.[1,17] Nearly half of the 74 anomalous properties of water listed by Chaplin are related to the polyamorphism, and they play remarkably important roles in various processes of the Earth.[17] Exploration of the water anomalies is therefore important for many research fields of science.

When two phases coexist, the chemical potential of one phase is the same as that of the other phase, but the potential energies are different from each other. One of the two phases must be more disordered than the other to compensate for the higher potential energy. In the case of the liquid-liquid phase transition of water models, the low-density liquid (LDL) and high-density liquid (HDL) phases correspond to the ordered and disordered ones, respectively. Although LDL does not possess any crystalline order, almost all water molecules are four-coordinated and its tetrahedral local structure is quite similar to ice. The structure of LDL is therefore often referred to as "icelike". This is, however, misleading. Topological analyses of the hydrogen bond network demonstrate that the intermediate-range order of ice is completely different from that of LDL.[18,19]

The distribution of the dihedral angle formed by four hydrogen bonding water molecules can be adopted to distinguish the difference between ice and supercooled liquid water. The angle can be defined in the same way as alkanes because both sp^3 carbon and water prefer tetrahedral network structures. Nguyen and Molinero

introduced a local order parameter, named CHILL+, to identify several ices that are stable under ambient pressures based on the tetrahedrality of the local structure.[20] Matsumoto *et al.* showed that there is a distinct difference in the dihedral distribution between ice and supercooled liquid water.[21]

In this paper, we propose a simple order parameter for water and ice named "twist" focusing on the dihedral angle. The twist order parameter is an extended version of the bond twist order parameter given in our previous work.[21] The twist parameter can distinguish LDL from HDL as well as ice Ic from Ih. The new order parameter is convenient, especially when two or more of the four phases coexist in a simulation box. Fine tunings of variables and criteria are not necessary for classification of water molecules because of the use of Bayesian decision theory.

DEFINITION OF TWIST

The atomic configuration around a water molecule is considered in most order parameters for water.[22–26] Our new order parameter, "twist", is not defined for each molecule but for each pair of water molecules forming a hydrogen bond, i and j, as

$$\chi_{ij} = \frac{1}{(M-1)(N-1)} \sum_{k=1}^{M-1} \sum_{l=1}^{N-1} \exp\left(3i\theta_{kijl}\right) \quad (\chi \in \mathbb{C}, |\chi| \le 1), \tag{1}$$

where k and l are water molecules that are hydrogen-bonded to molecules i and j, respectively, and M and N are the numbers of hydrogen bonds of water i and j. Typically, both M and N are 4 in ice. θ_{kijl} is the dihedral angle formed by four water molecules, k, i, j, and l, in sequence. A sample Python implementation is available in a GitHub repository.[27] We discussed how to define hydrogen bonds in water appropriately in a previous paper.[28] Properties on the hydrogen bond network including χ do not depend strongly on the structural parameters (e.g., O–O distance, O–H distance, and O–O–H angle) and the threshold values to determine a hydrogen bond when they are properly chosen. In this study, two water molecules are defined to be hydrogen-bonded when the shortest intermolecular O–H distance between them is less than 2.45 Å.[28]

In the diamond structure of ice Ic, any dihedral angle is either $\pi/3$, π, or $5\pi/3$ because of the staggered conformation, and so we obtain $\chi = -1$ (Fig. 1). In ice Ih, the dihedral angle for a hydrogen bond that is parallel to the c axis is either 0, $2\pi/3$, or $4\pi/3$ because of the eclipsed conformation. Thus, its twist value is 1 for any of the above angles. The imaginary part of χ is nonzero except for those special conformations. The twist parameter can be close to a purely imaginary number. We call conformations with $\chi = i$ and $-i$ the R-twisted and L-twisted conformations, respectively. In a previous study, we observed that clusters of the R-twisted configurations and those of the L-twisted configurations form in supercooled water because of the structural mismatch between the two types of twisted configurations.[21] In ambient conditions, such clusters do not form because the hydrogen bond network is flexible and distorted due to the thermal energy. The numbers of hydrogen bonds, M and N, are not always four for a water molecule, and there is structural incoherence in terms of the twist (i.e., the torsional angles for a hydrogen bond, θ_{kijl}, are not always twisted in the same direction).

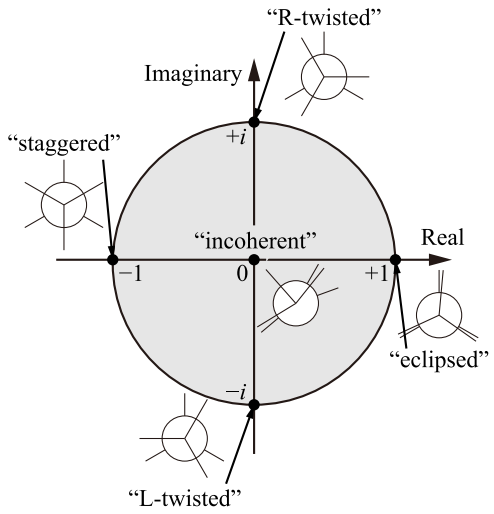

FIG. 1. Typical conformations shown in the Newman projection[29] and the corresponding values in the complex plane. The domain of the parameter χ is shown by the gray area.

As a result, both the real and imaginary parts of χ become close to zero.

The probability distributions of the twist χ for liquid water, ice Ih, and ice Ic are shown in Fig. 2. The TIP4P/2005 water model[5] is employed, and molecular dynamics (MD) simulations are performed at 1 bar using the GROMACS 4.6 package to generate molecular configurations in equilibrium states.[30,31] The initial structures of ice Ic and ice Ih are prepared using the GenIce tool.[32] They are relaxed at the target temperature and pressure. The temperature of an ice structure is elevated to 400 K with the volume fixed to melt it, and then it is annealed at a constant pressure, 1 bar, to obtain the liquid structures of target temperatures. The melting point of TIP4P/2005 water is 250 K.[33] The distributions for liquid water at the melting point, T_m, is similar to that at T_m + 30 K: there is a peak at $\chi' = 0$ and $\chi'' = 0$, where χ' and χ'' are the real and imaginary parts of χ, respectively. This peak, however, becomes less pronounced in supercooled water at T_m − 30 K and T_m − 60 K. There are two peaks in the distribution for ice Ih. The peak at $\chi' = -1$ arises from the hydrogen bonds forming 6-membered rings with the chair conformation, and the peak at $\chi' = 1$ is due to the hydrogen bonds that are parallel to the c-axis. There is only one peak in the distribution for ice Ic, reflecting that all hydrogen bonds in this ice are equivalent.

It is often possible to distinguish two phases even with the projection of χ on either the real or imaginary axis. For example, the difference between ice Ih [Fig. 2(e)] and LDL-like water[34] at T_m − 60 K [Fig. 2(a)] is obviously seen in the projection on the imaginary axis.[21] The difference between ice Ic [Fig. 2(f)] and Ih [Fig. 2(e)] is evident when the projections on the real axis are compared because of the eclipsed conformation that exists only in ice Ih.[35] The projection on the real axis for LDL-like water is asymmetric, as shown in Fig. 2(a). This tendency is found for the continuous random network that is a model of tetravalent network-forming

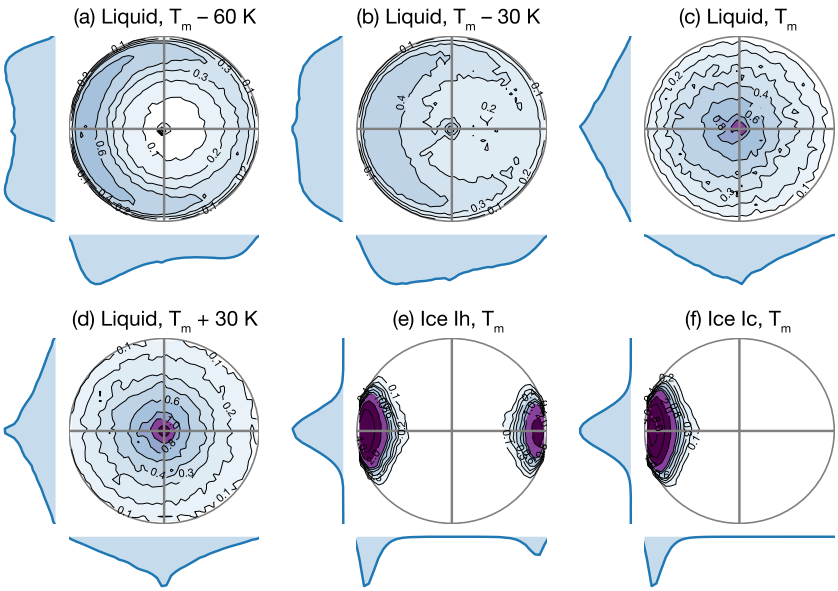

FIG. 2. Distributions of the twist parameter for liquid water and ices at ambient pressure. [(a)–(d)] Liquid water at 190 K (LDL-like), 220 K, 250 K, and 280 K (HDL-like). [(e) and (f)] Ices Ih and Ic at the melting point of the TIP4P/2005 water model, 250 K. Every 2D distribution accompanies two 1D functions each of which is the projection on the real and imaginary axes, respectively.

materials such as amorphous silicon and germanium,[36] suggesting that it would be a common geometric characteristic for this type of network.[18,19,37]

The distribution of liquid water at 220 K [Fig. 2(b)] can be represented by a linear combination of that at 250 K [Fig. 2(c)] and that at 190 K [Fig. 2(a)]. This implies that old "two-state" models of water that hypothesize liquid water as a mixture of two different types of molecules are a good description in terms of the twist.[38–40]

LIKELIHOOD ESTIMATED USING BAYESIAN THEORY

We assign a hydrogen bond to one of the four possible phases using the twist value. Bayes statistics provides us a useful framework for this.

Here, we assume that there are N different possible phases, $\{F_1, F_2, \ldots, F_N\}$. We have the probability density function of the twist χ for any single phase system out of all N phases (Fig. 2). The distribution function for the ith phase is expressed as $p(\chi|F_i)$. What we would like to know is the likelihood for a hydrogen bond in a target system with a value of the twist, χ, to be classified as one in phase F_i, i.e., $p(F_i|\chi)$, without any *a priori* knowledge on the target system except for phases that can exist in the system. The two probabilities can be connected using Bayes' theorem[41]

$$p(F_i|\chi) = \frac{p(\chi|F_i) \cdot p(F_i)}{p(\chi)}, \tag{2}$$

where $p(F_i)$ is the marginal probability for a randomly chosen hydrogen bond to be classified to a bond in phase F_i in the target system and $p(\chi)$ is the marginal probability density of χ in the target system. We assume that there are one or more domains in the target system, each of which corresponds to one of the possible phases. In this case, the twist distribution $p(\chi)$ can be expressed by a linear combination of $p(\chi|F_i)$ with $p(F_i)$ via the law of total probability

$$p(\chi) = \sum_i^N p(\chi|F_i)p(F_i). \tag{3}$$

The weight $p(F_i)$ is obtained from $p(\chi)$ and $p(\chi|F_i)$ using linear regression. When the target system is nonstationary, $p(F_i|\chi)$ can be dependent on time as a result of the changes in $p(\chi)$ and $p(F_i)$ with evolving times.

There are several limitations to this method: (1) Equation (3) is valid when the local structure in a domain of the ith phase in the target system is similar to that in the corresponding single phase system; (2) the weight $p(F_i)$ is obtained by linear regression, but this may be incorrect when the volume of the interfacial regions is not negligible; and (3) this method is applicable only when all possible phases are known in advance.

We apply the analysis protocol to an MD trajectory in which the four phases, ice Ih, ice Ic, HDL, and LDL, coexist. In a previous paper, we performed isothermal-isochoric (NVT) MD simulations of ST2 water and found that liquid water separates into HDL and LDL spontaneously and quickly at temperatures lower than the liquid-liquid critical point.[15] Ice nucleation inside the LDL domain occurred after the liquid-liquid separation in five simulations. We choose one of the five simulations as the target system. The simulation was performed at 0.98 g cm^{-3}. Liquid water was equilibrated at 300 K, and then the temperature was dropped to 235 K. The time of the temperature change was defined as $t = 0$. Here, we employ the ST2 water model instead of TIP4P/2005, although the latter is a better model to reproduce the thermodynamic properties of water because the ice nucleation rate of the ST2 model is fast enough to observe the formation of ice in LDL that coexists with HDL in MD simulations and, therefore, it is suitable for demonstration of the ability of the order parameter.

The twist distribution function $p(\chi|F_i)$ required for the linear regression is calculated from a single-phase MD simulation at the same temperature as the target system. The twist

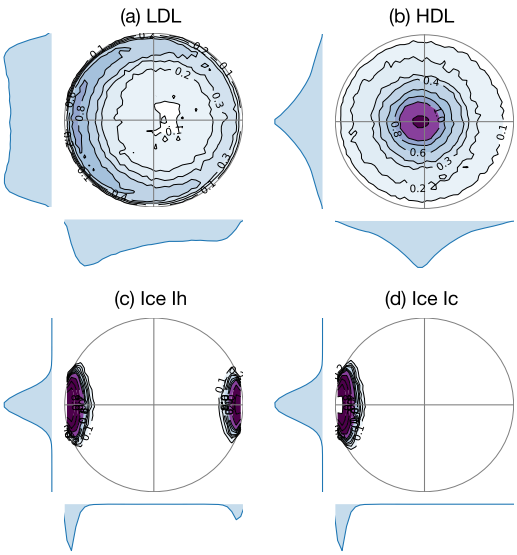

FIG. 3. The twist distributions of pure systems, $p(\chi|F_i)$, for the ST2 water model at 235 K. (a) LDL at 0.88 g cm^{-3}, (b) HDL at 1.04 g cm^{-3}, (c) ice Ih at 1 bar, and (d) ice Ic at 1 bar.

distributions for HDL and LDL, $p(\chi|\text{HDL})$ and $p(\chi|\text{LDL})$, are calculated at 1.04 g cm^{-3} and 0.88 g cm^{-3}, respectively, and those for ices Ic and Ih, $p(\chi|\text{Ic})$ and $p(\chi|\text{Ih})$, are calculated at 1 bar. These distributions are shown in Fig. 3.

Figure 4 shows the time evolution of the weight of the target system, $p(F_i)$, obtained by linear regression using Eq. (3). Liquid water under ambient conditions is HDL-like. The fraction of these types of hydrogen bonds, $p(\text{HDL})$, decreases, while that of LDL, $p(\text{LDL})$, increases immediately after the temperature drop at $t = 0$, indicating that liquid-liquid phase separation occurs very quickly. This fast separation is caused by the absence of mass transfer that is necessary for usual liquid-liquid separation processes such as oil-water separation. The number of icelike hydrogen bonds is very

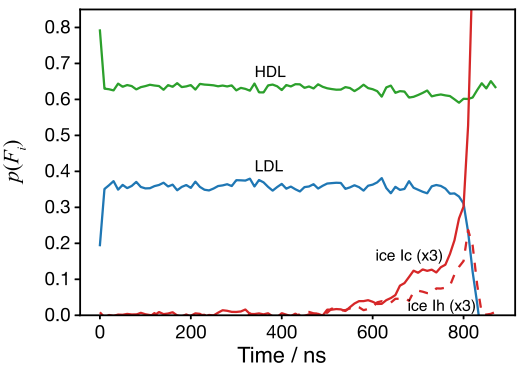

FIG. 4. Time evolution of the fraction of each phase, $p(F_i)$, for the target MD trajectory in which liquid-liquid separation and ice nucleation occur. The curves for Ic and Ih are vertically magnified for clarity.

small until $t = 500$ ns at which an ice nucleus reaches the critical size. The ice nucleus is not a single crystal but a complex of ice Ih and Ic fragments. An ice Ic fragment begins to grow very quickly at $t = 800$ ns because its size exceeds the shortest dimension of the simulation box.

Comparison with various local structure indices (tetrahedrality, q_{tet},[42] distance to the 5th nearest neighbor, g_5,[25] and the gap between the 1st and the 2nd shells, ζ[26]) are given in Fig. S1 of the supplementary material. These order parameters are less sensitive to the emergence of ice nuclei in liquid.

VISUALIZATION WITH THREE COLORING SCHEMES

We obtain four likelihood values for a χ value, i.e., $p(\text{Ih}|\chi)$, $p(\text{Ic}|\chi)$, $p(\text{HDL}|\chi)$, and $p(\text{LDL}|\chi)$, using Eq. (2). Plotting them separately on four complex planes is not informative. We plot the four likelihood functions in one complex plane assigning a color to each phase. We ignore the difference between ices Ih and Ic for simplicity and define the probability for ice I as

$$p(\text{Ice}|\chi) = p(\text{Ic}|\chi) + p(\text{Ih}|\chi). \tag{4}$$

The assigned colors to ice I, HDL, and LDL are red, green, and blue, respectively. The color for a value of χ is made by mixing the three colors, considering the probabilities $p(F_i|\chi)$. For example, if we have $p(\text{Ice}|\chi) = 0.5$, $p(\text{HDL}|\chi) = 0.0$, and $p(\text{LDL}|\chi) = 0.5$, the color for this χ value is dark purple which is a mixed color of red and blue. We call this scheme the color mixing (CM) scheme. Figure 5(a) shows the likelihood calculated from the target MD trajectory for a time window ranging from 750 ns to 780 ns during which ice I, LDL, and HDL coexist in the simulation box. The color of the region between red (ice) and blue (LDL) is dark purple.

The χ value is calculated for every hydrogen bond. Therefore, we can draw snapshots of the MD trajectory in which the likelihood of a bond is represented by a mixed color. Such snapshots are shown in the top panels of Fig. 6. Most hydrogen bonds are HDL-like at $t = 0$. The system is divided into an HDL domain and an LDL domain at $t = 10$ ns. There is an ice nucleus in the LDL domain at $t = 600$ ns, and it grows as time evolves.

The use of mixed colors may not be helpful in actual applications. We reduce colors by representing a χ value with the color of the most likely phase. The likelihood $p(F_i|\chi)$ can be small even

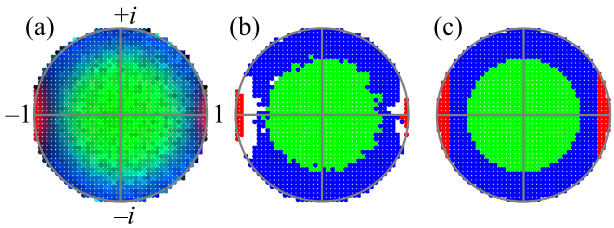

FIG. 5. Likelihood calculated from the target MD trajectory for a time window ranging from 750 ns to 780 ns plotted with the (a) CM scheme, (b) DB scheme, and (c) SB scheme. A hydrogen bond with a χ value in the red, green, and blue areas in the figure is more likely to be in the ice, HDL, and LDL domains in the target system.

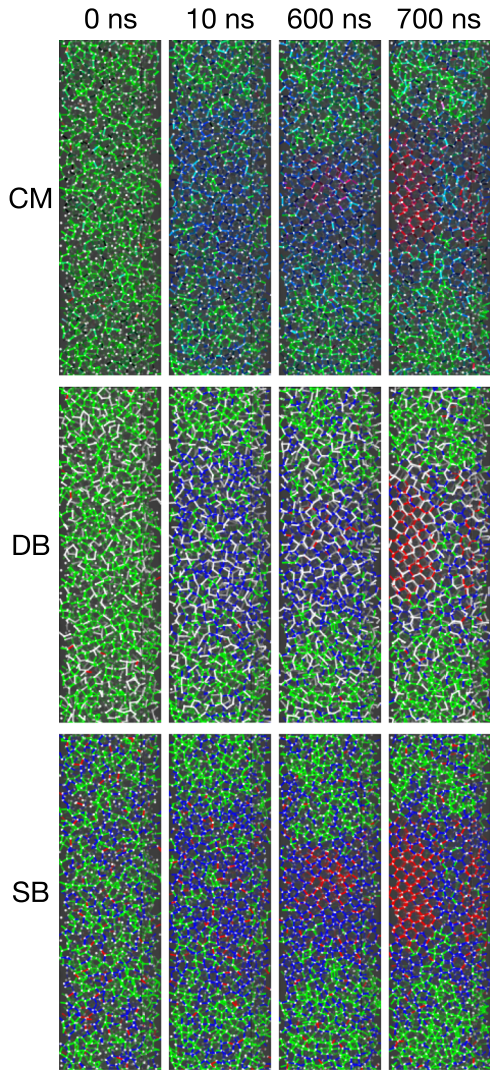

FIG. 6. Hydrogen bond network of water at t = 0, 10, 600, and 700 ns colored with the (top) CM scheme, (middle) DB scheme, and (bottom) SB scheme. Red, green, and blue bonds represent hydrogen bonds in ice I, HDL, and LDL, respectively. A rectangular simulation box is employed so that the liquid-liquid interface formed in the box becomes perpendicular to the longest axis to minimize the surface area.[15]

for the most likely phase for χ values that are possible in many phases. We assign white to χ values at which the largest $p(F_i|\chi)$ is less than 0.5. Figure 5(b) is the map based on this scheme. The decision boundaries (DB) are shown in this map. The dark purple region in Fig. 5(a) is now left blank because the most likely phase is undecidable. We call this scheme the DB coloring scheme. The middle panels of Fig. 6 show snapshots colored with the DB scheme.

It is possible to classify hydrogen bonds of a different trajectory using Fig. 5(b) when its thermodynamic condition is not so different from that of the MD trajectory used to obtain Fig. 5(b). For such an application, it may be more useful when the DBs are represented by smooth curves in the complex plane. The boundaries between LDL (blue) and ice (red) in Fig. 5(c) are approximated by vertical lines at $\chi' = 0.85$ and -0.85, ignoring the white regions, and the boundary between LDL (blue) and HDL (green) is approximated by a circle with a radius of 0.65 [Fig. 5(c)]. The snapshots colored with this scheme, which we call the simplified boundary (SB) scheme, are shown in the bottom panels of Fig. 6. Each domain is more distinctive for the SB scheme than for the CM scheme.

CONCLUSION

We introduce a minimalistic order parameter for water named twist to distinguish ice Ih, ice Ic, LDL, and HDL. The values of this parameter fall in the unit circle centered at the origin in the complex plane. The likelihood for a hydrogen bond in a target system with a value of the twist to be classified as a bond in one of the possible phases is estimated according to Bayes' theorem. Three coloring schemes are proposed for visualization of MD trajectories on the basis of the likelihood. Domains of different phases are clearly distinguished by the present method for a MD trajectory in which ice nucleation occurs after liquid-liquid separation in the deeply supercooled condition.

The twist parameter will be useful to screen the local structures of water that appear in confined systems and near material surfaces. The twist parameter is also useful to detect the chiral heterogeneity in the local structure that is remarkable in supercooled liquid water.[21]

One can design more complicated order parameters for more exquisite classification of local structures of water. The twist order parameter distinguishes ices Ic and Ih in a probabilistic manner because it is defined for a single bond. It would be possible to find a new order parameter that allows us to distinguish the two or more ice phases as well as clathrate hydrates in a more deterministic way considering the correlation between the twist values of the neighboring hydrogen bonding pair. The Bayesian approach would also be a powerful tool to classify local structures with such a complicated order parameter and to evaluate its performance.

The use of the torsional angle is not very suitable for classification of high-pressure ice phases, such as ice III and VI, because their hydrogen bond networks are highly distorted. Analyses based on topological structures such as rings and polyhedra would be better to identify the intermediate-range order in the high-pressure phases of water.[19]

SUPPLEMENTARY MATERIAL

See supplementary material for analyses using various conventional local structure indices.

ACKNOWLEDGMENTS

The present work was supported by a grant of MORINO FOUNDATION FOR MOLECULAR SCIENCE and JSPS KAKENHI Grant No. 16K05658 and MEXT as "Priority Issue on Post-Kcomputer" (Development of new fundamental technologies for high-efficiency energy creation, conversion/storage and use). MD simulations were performed on the computers at the Research Center for Computational Science, Okazaki, Japan.

REFERENCES

[1] P. Ball, *H_2O: A Biography of Water* (Hachette, UK, 2015).
[2] A. Rahman and F. H. Stillinger, J. Chem. Phys. **55**, 3336 (1971).
[3] E. Sanz, C. Vega, J. L. F. Abascal, and L. G. MacDowell, Phys. Rev. Lett. **92**, 255701 (2004).
[4] E. Sanz, C. Vega, J. L. F. Abascal, and L. G. MacDowell, J. Chem. Phys. **121**, 1165 (2004).
[5] J. L. F. Abascal and C. Vega, J. Chem. Phys. **123**, 234505 (2005).
[6] C. Vega, J. L. F. Abascal, M. M. Conde, and J. L. Aragones, Faraday Discuss. **141**, 251 (2009).
[7] M. M. Conde, C. Vega, G. A. Tribello, and B. Slater, J. Chem. Phys. **131**, 034510 (2009).
[8] A. Falenty, T. C. Hansen, and W. F. Kuhs, Nature **516**, 231 (2014).
[9] X. Fan, D. Bing, J. Zhang, Z. Shen, and J.-L. Kuo, Comput. Mater. Sci. **49**, S170 (2010).
[10] C. Knight, S. J. Singer, J.-L. Kuo, T. K. Hirsch, L. Ojamäe, and M. L. Klein, Phys. Rev. E **73**, 056113 (2006).
[11] O. Mishima, L. D. Calvert, and E. Whalley, Nature **314**, 76 (1985).
[12] O. Mishima, Nature **384**, 546 (1996).
[13] O. Mishima and H. Eugene Stanley, Nature **396**, 329 (1998).
[14] P. H. Poole, F. Sciortino, U. Essmann, and H. Eugene Stanley, Nature **360**, 324 (1992).
[15] T. Yagasaki, M. Matsumoto, and H. Tanaka, Phys. Rev. E **89**, 020301 (2014).
[16] J. C. Palmer, P. H. Poole, F. Sciortino, and P. G. Debenedetti, Chem. Rev. **118**, 9129 (2018).
[17] M. F. Chaplin, Anomalous Properties of Water, Water Structure and Science, http://www1.lsbu.ac.uk/water/water_anomalies.html, 2019.
[18] R. Alben and P. Boutron, Science **187**, 430 (1975).
[19] M. Matsumoto, A. Baba, and I. Ohmine, J. Chem. Phys. **127**, 134504 (2007).
[20] A. H. Nguyen and V. Molinero, J. Phys. Chem. B **119**, 9369 (2015).
[21] M. Matsumoto, T. Yagasaki, and H. Tanaka, Phys. Rev. Lett. **115**, 197801 (2015).
[22] J. R. Errington, P. G. Debenedetti, and S. Torquato, Phys. Rev. Lett. **89**, 215503 (2002).
[23] G. Ruocco, M. Sampoli, and R. Vallauri, J. Mol. Struct. **250**, 259 (1991).
[24] P. J. Steinhardt, D. R. Nelson, and M. Ronchetti, Phys. Rev. Lett. **47**, 1297 (1981).
[25] M. J. Cuthbertson and P. H. Poole, Phys. Rev. Lett. **106**, 115706 (2011).
[26] J. Russo and H. Tanaka, Nat. Commun. **5**, 3556 (2014).
[27] M. Matsumoto, A GitHub Repository, https://github.com/vitroid/twist-op, 2019.
[28] M. Matsumoto, J. Chem. Phys. **126**, 054503 (2007).
[29] M. S. Newman, J. Chem. Educ. **32**, 344 (1955).
[30] D. Van Der Spoel, E. Lindahl, B. Hess, G. Groenhof, A. E. Mark, and H. J. C. Berendsen, J. Comput. Chem. **26**, 1701 (2005).
[31] B. Hess, C. Kutzner, D. van der Spoel, and E. Lindahl, J. Chem. Theory Comput. **4**, 435 (2008).
[32] M. Matsumoto, T. Yagasaki, and H. Tanaka, J. Comput. Chem. **39**, 61 (2018).
[33] M. M. Conde, M. Rovere, and P. Gallo, J. Chem. Phys. **147**, 244506 (2017).
[34] J. L. F. Abascal and C. Vega, J. Chem. Phys. **133**, 234502 (2010).
[35] E. B. Moore and V. Molinero, Phys. Chem. Chem. Phys. **13**, 20008 (2011).
[36] D. E. Polk, J. Non-Cryst. Solids **5**, 365 (1971).
[37] V. Molinero and E. B. Moore, J. Phys. Chem. B **113**, 4008 (2009).
[38] W. C. Röntgen, Ann. Phys. Chem. **281**, 91 (1892).
[39] G. E. Walrafen, M. S. Hokmabadi, and W.-H. Yang, J. Chem. Phys. **85**, 6964 (1986).
[40] C. A. Angell and V. Rodgers, J. Chem. Phys. **80**, 6245 (1984).
[41] T. Bayes, R. Price, and J. Canton, "An Essay Towards Solving a Problem in the Doctrine of Chances," in *The Philosophical Transactions of the Royal Society of London* (Royal Society Publishing, 1763), Vol. 53, p. 370.
[42] J. R. Errington and P. G. Debenedetti, Nature **409**, 318 (2001).